Correlation between Structural Order and Diffusion Length in Granular Flow

David Luce,[1,2,*] Adrien Gans,[1] Sébastien Kiesgen De Richter,[1,3] and Nicolas Vandewalle[2]

[1] *LEMTA, Université de Lorraine, CNRS, 2, Avenue de la Forêt de Haye, Vandœuvre-lès-Nancy, 54504, France*
[2] *GRASP, Institute of Physics B5a, Université de Liège, 4000 Liège, Belgium*
[3] *Institut Universitaire de France (IUF)*

We investigate how structural ordering, i.e. crystallization, affects the flow of bidisperse granular materials in a quasi-two-dimensional silo. By systematically varying the mass fraction of two particle sizes, we finely tune the degree of local order. Using high-speed imaging and kinematic modeling, we show that crystallization significantly enhances the diffusion length b, a key parameter controlling the velocity profiles within the flowing medium. We reveal a strong correlation between b, the hexatic order parameter ψ_6 and the cluster size ξ, highlighting the role of local structural organization in governing macroscopic flow. Furthermore, pressure gradients within the silo stabilize orientational order even without crystallization, thus intrinsically increasing b with height. These results highlight a direct link between microstructural order, pressure, and transport properties in granular silo flows, and suggest that similar mechanisms may operate in other particulate systems, such as colloids, foams, or emulsions, where local structural ordering and confinement affect flow and transport.

Dense collections of particles, from colloidal suspensions to granular assemblies, exhibit a rich variety of collective phenomena driven by geometric constraints and interparticle interactions. Granular materials provide a particularly simple and versatile model to investigate fundamental aspects of structural organization. Composed of discrete macroscopic particles, granular media display a wide range of collective behaviors that often defy intuition due to their athermal nature and dissipative interactions. Among these behaviors, structural ordering is a central aspect [1]. When monodisperse spherical grains are densely packed, they tend to self-organize into highly ordered configurations, such as hcp and fcc lattices, which represent efficient packing arrangements [2]. However, even slight size polydispersity can disrupt this tendency, preventing crystallization and promoting disordered or amorphous structures that lack long-range translational order [3–5]. This effect is particularly pronounced in two-dimensional systems, where monodisperse disks spontaneously form hexagonal crystallites under confinement that shrink when a second species is inserted (see Fig. 1(a-d)).

While it is well established that stresses in granular media propagate along discrete contact networks, the influence of structural order on this transmission, particularly under flow conditions, remains a complex and actively debated topic [3, 4, 6–11]. To suppress undesired ordering effects, especially in experimental investigations of flow, compaction, or jamming, bidisperse mixtures are commonly used [3, 7]. This strategy prompts several fundamental questions: which combinations of grain size ratios and mixing fractions most effectively hinder crystallization, and to what extent does the presence or absence of local structural order modify the mechanical response and dynamical behavior of granular systems?

The quasi-two-dimensional silo provides an ideal framework to investigate the interplay between particle ordering and granular flow. Over the past decades,

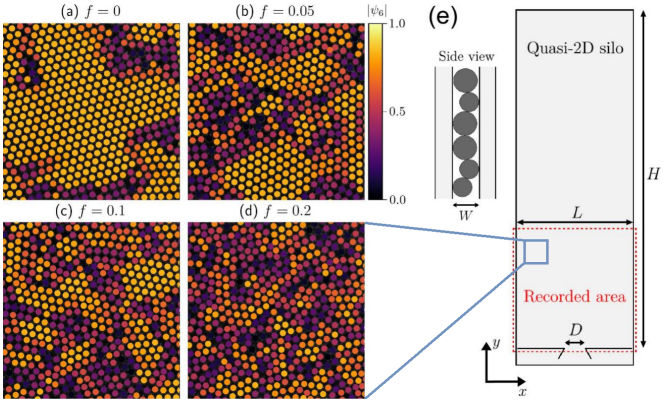

FIG. 1. Four snapshots of the bidisperse granular media in a discharging 2D silo for different values of the mass fraction of small particles (a) $f = 0$, (b) $f = 0.05$, (c) $f = 0.1$ and (d) $f = 0.2$. Each particle is colored according to the hexatic order parameter modulus $|\psi_6|$ given by Eq. (1) from yellow (order) to dark (disorder). (e) Sketch of the experimental quasi-2D silo with relevant parameters. The red dashed rectangle represents the filmed area (10 cm × 10 cm).

granular discharge from silos has been extensively studied, leading to the development of several semi-empirical models that capture key flow properties such as the discharge rate [12–14], the internal velocity field [15–19], and the dynamics near the outlet [14, 20]. Despite this knowledge, the influence of structural ordering, particularly crystallization, within the bulk reservoir of the silo remains largely unexplored. This gap motivates a detailed investigation of how local particle arrangements affect the flow behavior in bidisperse systems.

We designed a quasi-two-dimensional, flat-bottom silo similar to that of [21], confining the grains to a single monolayer (see Fig. 1(e)). The polycarbonate walls are coated with a conductive layer to reduce triboelectric charging. The cell dimensions are $H = 300$ mm (height), $L = 100$ mm (width), and $W = 1.25$ mm (depth), with a fixed outlet width of 18 mm. The granu-

lar medium is a binary mixture of steel spheres with diameters $d_1 = 1.0 \pm 0.01$ mm and $d_2 = 1.2 \pm 0.01$ mm, and we define the average reference diameter as $d = 1.1$ mm. This slight size difference suppresses segregation effects [22]. The mass fraction of small beads is denoted by f, corresponding to the proportion of 1.0 mm particles in the mixture. Opening the aperture by lifting a retaining wire initiates the flow, enabling us to investigate discharge dynamics as a function of f. For each value of f, five independent discharge experiments were conducted. The flow was recorded at 2000 frames per second using a high-speed camera. Each video, with a resolution of 1024×1024 pixels (corresponding to a physical area of $91\,d \times 91\,d$, see Fig. 1), focuses on the bottom region of the silo during the steady-state discharge. Lagrangian particle data are projected onto an Eulerian grid of square cells of size $d \times d$, whose bottom-central cell is aligned with the center of the outlet. Eulerian fields of any measurable quantity are obtained by averaging the corresponding Lagrangian values of all particles intersecting a given cell at position (x, y).

Fig. 1(a–d) presents snapshots of the granular packings within the silo for four different values of f, ranging from the monodisperse case ($f = 0$) to a low fraction of small particles ($f = 0.2$). Grains are color-coded according to their local structural environment, from crystalline regions (yellow) to amorphous ones (dark). To quantify this local order, we compute for each particle k the hexatic order parameter based on the angular positions $\theta_{k\ell}$ of its N_k nearest neighbors

$$\psi_{6k} = \frac{1}{N_k} \sum_{\ell=1}^{N_k} \exp\left(i 6 \theta_{k\ell}\right), \qquad (1)$$

where $|\psi_{6k}|$ close to 1 indicates a strong sixfold symmetry typical of hexagonal packing. The images clearly show that the large crystalline domains observed at $f = 0$ are rapidly disrupted as f increases, giving way to smaller clusters and disordered regions. This confirms that bidispersity suppresses long-range order and promotes amorphous configurations.

A second structural measure confirms these observations. A Voronoi tessellation is applied to all grains, assigning to each grain k a Voronoi cell of area A_k. We compute the Probability Distribution Function (PDF) of the dimensionless areas A/d^2 for various values of f, as shown in Fig. 2. For the monodisperse case ($f = 0$), only large grains are present and the distribution is sharply peaked. As f increases, a second peak emerges at smaller normalized areas, indicating the inclusion of smaller grains. The overall distribution broadens, reaching its widest spread near $f = 0.5$, before narrowing again for high f values. At $f = 1$, where only small particles are present, crystalline domains reappear, although the peak remains broader than in the $f = 0$ case. This is due to the limited confinement imposed by the silo geometry, governed

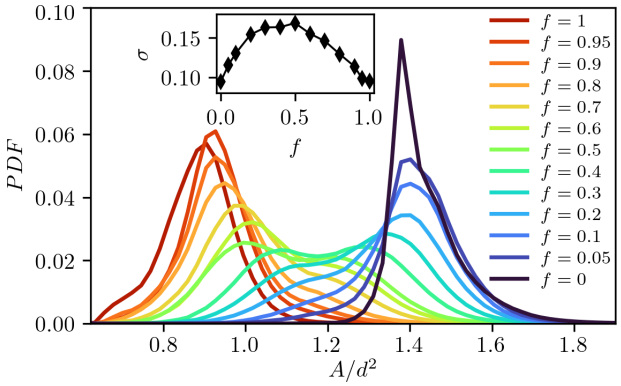

FIG. 2. Probability Distribution Function of Voronoi cell areas A normalized by a typical grain area d^2. Different mixing fractions f produce distinct bimodal distributions. Inset: standard deviation of each distribution σ versus f.

by the grain-to-width ratio W/d. When W/d deviates from the ideal value $W/d = 1$, particle overlap occurs, leading to a reduction of positional order. In monodisperse systems, W/d takes the values 1.04 ($f = 0$) and 1.25 ($f = 1$), both of which are nevertheless sufficient to allow the formation of crystalline structures. The inset of Fig. 2 shows the standard deviation of the PDFs, which is minimal for $f = 0$ and $f = 1$, consistent with the emergence of crystallization in the system. Conversely, it reaches a maximum around intermediate values of f, in agreement with an amorphous regime.

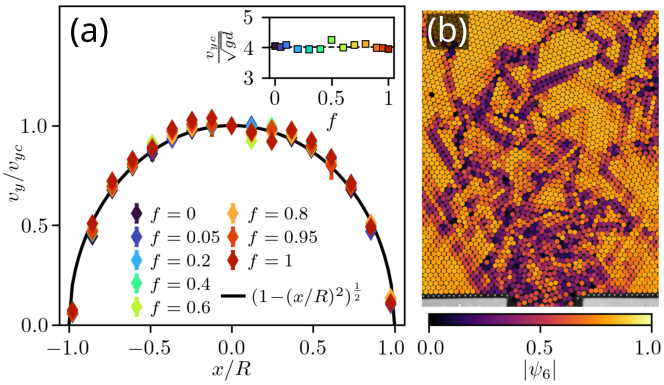

FIG. 3. (a) Normalized vertical velocity v_y/v_{yc} profiles for all mixing fractions f. The black line corresponds to the fitting from [14], $\left(1 - (x/R)^2\right)^{1/2}$, with R the radius of the silo aperture. The inset presents the central velocity v_{yc} normalized by the characteristic speed $\sqrt{gd}$, emphasizing no significant dependency of the mixing fractions f. (b) Snapshot of the amorphous granular media for $f = 0$ near the outlet.

The above results are confirming the validity of most experimental protocols in which binary mixtures are used to avoid crystallization. The next relevant question is to measure the effect of this mixture on the global granular flow. In particular, we compute the average vertical velocity field $v_y(x, y)$ as a function of the mixing fraction

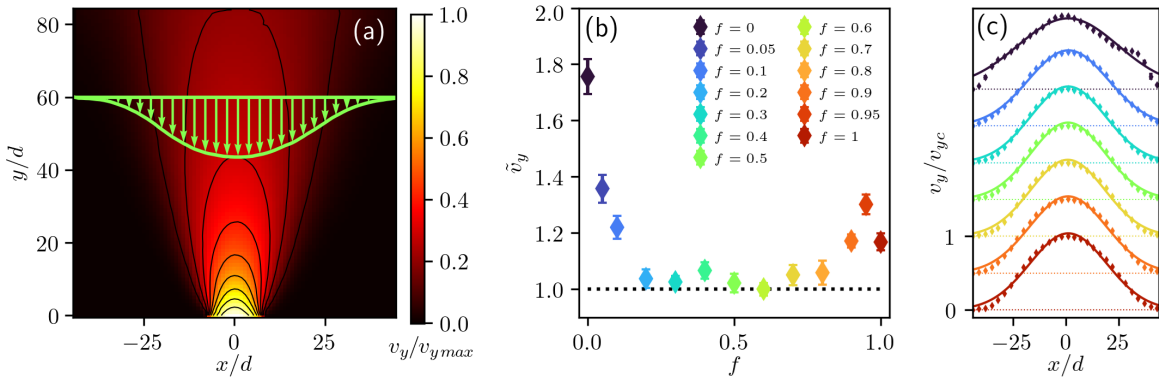

FIG. 4. (a) Time-averaged normalized vertical velocity field $v_y/v_{y\,\max}$ at $f = 0.5$. The velocity profile $v_y(x)$ at $y/d = 60$ is highlighted in green. (b) Reduced vertical velocity near the sheared zone, $\tilde{v}_y(f) = v_y(x_0, y_0; f)/v_y(x_0, y_0; 0.5)$, evaluated at $(x_0, y_0) = (30d, 60d)$. (c) Bulk normalized vertical velocity profiles for mixing fractions $f \in [0, 1]$. The profiles are vertically offset for clarity, with horizontal dotted lines of the same color indicating the zero level. Solid lines correspond to fits of Eq. (2).

f. Let us start by the outlet of the silo where the velocity profiles exhibit no significant dependence on f, in agreement with prior observations reported in [11, 14] (see Fig. 3(a)). The expected profile around the outlet is fitted to all data. Fig. 3(b) shows that particles near the outlet have lower $|\psi_6|$ values than those higher up in the flow for $f = 0$. Even in the crystallization regime, this indicates that orientational correlations vanish in this dilute region, where the granular medium experiences a strong pressure drop [23].

However, the effect of mixing granular species can be observed in the silo far from the outlet. A typical velocity field $v(x, y)$ is shown in Fig. 4(a) where dead zones appear in dark colors, while fast-moving regions close to the outlet are shown in yellow. More precisely, Fig. 4(b) shows the vertical velocity in the transition zone between the solid-like and liquid-like regions for different f values. The onset of crystallization for $f = 0$ and $f = 1$ increases the velocity in this region, indicating enhanced momentum diffusion in the direction transverse to the flow.

Much of the granular material in the silo is in motion and this is well described by the kinematic model introduced by Nedderman and Tüzün [17], based on the earlier work of Litwiniszyn [15]. The model assumes that the medium is incompressible, i.e. $\partial_x v_x + \partial_y v_y = 0$, and that the horizontal velocity is proportional to the horizontal gradient of the vertical velocity, i.e. $v_x = b\,\partial_x v_y$. This leads to Gaussian-like-shaped vertical velocity profiles of the form

$$v_y(x, y) = \frac{-Q}{\sqrt{4\pi b y}} \exp\left(\frac{-x^2}{4by}\right), \qquad (2)$$

where Q is the time-averaged flow rate. The model introduces a single fitting parameter, b, which represents a characteristic diffusion length of the medium [19]. Fig. 4(c) shows the velocity profiles for $f \in [0, 1]$, taken at $y/d = 60$, for comparison. They can be well fitted by Eq. (2), demonstrating that the model captures the effects of crystallization on the flow, in particular the broadening of the velocity profile previously mentioned.

The characteristic diffusion length of the medium, b, can thus be extracted as a function of the height y/d and the mixing fraction f. Fig. 5 (a) shows resulting b/d values as a function of vertical position y/d. In the specific case of $f = 0$ and $y/d > 60$, the velocity profiles exhibit a plug-flow component caused by the presence of a large flowing cluster, preventing an accurate determination of b/d. The diffusion length b systematically increases with height within the silo. This trend is consistent with the observations of Medina et al. [18], who performed measurements in a monodisperse granular medium, under conditions where the aspect ratio between the silo gap and particle size W/d corresponds to our case with $f = 1$. Our results further show that the rate of increase of the diffusion length b is minimal near $f \approx 0.5$, corresponding to an amorphous state, and becomes significantly larger in the presence of structural ordering. Specifically, the diffusion length reaches a value of $b/d = 4.5$ in the most crystalline case ($f < 0.05$), which exceeds previously reported values for slightly polydisperse granular systems under similar conditions [16, 18, 24, 25]. This enhanced diffusivity is strongly correlated with the apparent clustering induced by crystallization. The organization into crystalline blocks leads to an enlargement of the set of mechanically stable configurations available to the grains, thereby reducing the occurrence of metastable, mechanically frustrated states. As a consequence, the likelihood of localized plastic events occurring during flow decreases, a mechanism suggested to underlie the anomalous diffusion behavior observed in granular media [26].

Since the presence of crystalline clusters affects flow properties, we measured their apparent diameter, ξ/d, as a function of their vertical position in the system (see Fig. 5(b)). We show that the blocks grow larger with height and as f approaches 0 or 1. This is directly related to the increase in pressure with height, which stabilizes the internal clustered structure and enhances the rigidity of the system. The size ξ/d follows the same trend as b/d, revealing the key role of crystallization in the momentum diffusion process in silo flow.

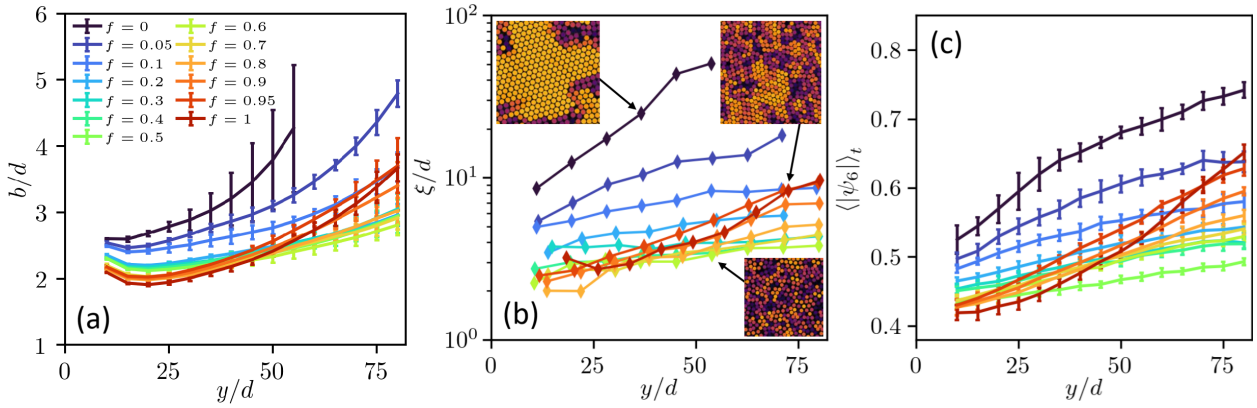

FIG. 5. Evolution of (a) the normalized parameter b/d in the silo, (b) the normalized crystal diameter ξ/d and (c) modulus of the local hexatic order parameter $\langle|\psi_6|\rangle_t$, as a function of height for $f \in [0, 1]$. ξ/d is estimated using a percolation-based method applied to the local modulus of the hexatic order parameter. Panel (b) shows three examples of internal structure for $f = 0$ (top left), $f = 1$ (top right), and $f = 0.5$ (bottom right), using the same colormap as in Fig. 1 and Fig. 3(b).

To further analyze the structural order, we compute the local time-averaged magnitude of the hexatic order parameter, $\langle|\psi_6|\rangle_t$, as an Eulerian field. Previous studies have established a link between dynamic heterogeneity and short-range orientational order [4]. While instantaneous $|\psi_6|$ reflects the presence of hexatic structures, the time-averaged field $\langle|\psi_6|\rangle_t$ is inversely correlated with the frequency of plastic rearrangements. Its values vary only weakly along the horizontal axis x, allowing averaging over $-15 \leq x/d \leq 15$, but increase significantly with height, as shown in Fig. 5(c). In high-velocity regions, $\langle|\psi_6|\rangle_t$ ranges between 0.41 and 0.52, indicating substantial dislocation activity. Conversely, higher in the silo, it reaches up to 0.75 in the fully crystalline case ($f = 0$), suggesting slower dynamics where plastic events are suppressed by both elevated pressure [27] and the structural ordering identified here. Velocity profiles measured at the outlet and in the bulk remain quantitatively similar as long as the observed value of $\langle|\psi_6|\rangle_t$ stays below the threshold $\langle|\psi_6|\rangle_t = 0.6$ [9]. Above this threshold, the profiles develop broader tails, which are well captured by the diffusion length b.

A clear correlation thus emerges between the diffusion length b and the local time-averaged degree of order $\langle|\psi_6|\rangle_t$, as shown in Fig. 6. A high rate of dislocations, reflected by low $\langle|\psi_6|\rangle_t$ values, results in poor diffusion, as momentum transfer is hindered by energy dissipation from plastic events mostly near the outlet. In contrast, a low dislocation rate, indicated by high $\langle|\psi_6|\rangle_t$ values, is associated with more efficient momentum propagation, a mechanism reinforced by increasing confining pressure, potentially explaining the rise in the global diffusion parameter b/d observed in previous studies [18].

In summary, we investigated how local structural ordering, i.e. crystallization, affects the flow of granular materials in a quasi-2D silo. Crystalline domains enhance local rigidity, facilitating momentum transfer and increasing the diffusion length b. A strong correlation between the hexatic order parameter and b highlights the pivotal role of microstructural organization in governing macroscopic flow. Even without significant crystallization, the pressure increase with height stabilizes local orientational order, gradually raising b. These findings point to pressure as a key factor mediating the interplay between structural order and transport properties in granular silo flows. They may also have broader implications for other particulate systems, such as colloidal suspensions, foams, or emulsions, where local structural ordering and confinement similarly affect flow and transport, suggesting a general connection between microstructural organization and macroscopic rheology.

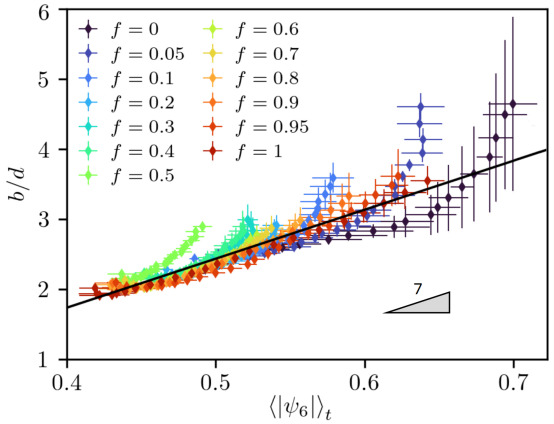

FIG. 6. Correlation between the local modulus of the hexatic order parameter $\langle|\psi_6|\rangle_t$ and the characteristic diffusion length b/d for $y/d \in [10, 80]$. The black line is a guide to the eye with slope 7 ($r = 0.85$ in the range $y/d \in [10, 80]$).

This work was partially supported by the LUE program of the University of Lorraine and by the Institut Universitaire de France (IUF), which significantly contributed to the achievement of this research.

* david.luce@uliege.be

[1] P. Schall, D. Weitz, and F. Spaepen, Structural rearrangements that govern flow in colloidal glasses, Science **318**, 1895 (2007).

[2] S. Torquato and F. H. Stillinger, Jammed hard-particle packings: From kepler to bernal and beyond, Reviews of modern physics **82**, 2633 (2010).

[3] G. Petekidis, A. Moussaid, and P. Pusey, Rearrangements in hard-sphere glasses under oscillatory shear strain, physical review E **66**, 051402 (2002).

[4] K. Watanabe and H. Tanaka, Direct observation of medium-range crystalline order in granular liquids near the glass transition, Physical review letters **100**, 158002 (2008).

[5] L. Kondic, A. Goullet, C. O'Hern, M. Kramar, K. Mischaikow, and R. Behringer, Topology of force networks in compressed granular media, Europhysics Letters **97**, 54001 (2012).

[6] P. M. Reis, R. A. Ingale, and M. D. Shattuck, Crystallization of a quasi-two-dimensional granular fluid, Physical review letters **96**, 258001 (2006).

[7] A. Lemaître and C. Caroli, Rate-dependent avalanche size in athermally sheared amorphous solids, arXiv preprint arXiv:0903.3196 (2009).

[8] M. Benyamine, M. Djermane, B. Dalloz-Dubrujeaud, and P. Aussillous, Discharge flow of a bidisperse granular media from a silo, Physical Review E **90**, 032201 (2014).

[9] J. Downs, N. Smith, K. Mandadapu, J. Garrahan, and M. Smith, Topographic control of order in quasi-2d granular phase transitions, Physical Review Letters **127**, 268002 (2021).

[10] J. Bai, J. Li, G. Hong, J. Pan, and H. Fei, Mesoscopic evolution and kinetic properties of dense granular flow crystallization under continuous shear induction, Powder Technology **426**, 118615 (2023).

[11] C. M. Carlevaro, R. Kozlowski, and L. A. Pugnaloni, Flow rate in 2d silo discharge of binary granular mixtures: the role of ordering in monosized systems, Frontiers in Soft Matter **4**, 1340744 (2024).

[12] G. H. L. Hagen, Über den druck und die bewegung des trocknen sandes, Bericht über die zur Bekanntmachung geeigneten Verhandlungen der Königlich Preussischen Akademie der Wissenschaften zu Berlin , 35 (1852).

[13] W. A. Beverloo, H. A. Leniger, and J. Van de Velde, The flow of granular solids through orifices, Chemical engineering science **15**, 260 (1961).

[14] A. Janda, I. Zuriguel, and D. Maza, Flow rate of particles through apertures obtained from self-similar density and velocity profiles, Physical review letters **108**, 248001 (2012).

[15] J. Litwiniszyn, An application of the random walk argument to the mechanics of granular media, Rheology and Soil Mechanics: Symposium Grenoble, April 1–8, 1964 , 82 (1964).

[16] W. Mullins, Experimental evidence for the stochastic theory of particle flow under gravity, Powder Technology **9**, 29 (1974).

[17] R. Nedderman and U. Tüzün, A kinematic model for the flow of granular materials, Powder Technology **22**, 243 (1979).

[18] A. Medina, J. Cordova, E. Luna, and C. Trevino, Velocity field measurements in granular gravity flow in a near 2d silo, Physics Letters A **250**, 111 (1998).

[19] J. Choi, A. Kudrolli, and M. Z. Bazant, Velocity profile of granular flows inside silos and hoppers, Journal of Physics: Condensed Matter **17**, S2533 (2005).

[20] M. Benyamine, P. Aussillous, and B. Dalloz-Dubrujeaud, Discharge flow of a granular media from a silo: effect of the packing fraction and of the hopper angle, EPJ Web of Conferences **140**, 03043 (2017).

[21] A. Pascot, J.-Y. Morel, S. Antonyuk, M. Jenny, Y. Cheny, and S. K. De Richter, Discharge of vibrated granular silo: A grain scale approach, Powder Technology **397**, 116998 (2022).

[22] L. A. Golick and K. E. Daniels, Mixing and segregation rates in sheared granular materials, Physical Review E—Statistical, Nonlinear, and Soft Matter Physics **80**, 042301 (2009).

[23] C. Perge, M. A. Aguirre, P. A. Gago, L. A. Pugnaloni, D. Le Tourneau, and J.-C. Géminard, Evolution of pressure profiles during the discharge of a silo, Physical Review E—Statistical, Nonlinear, and Soft Matter Physics **85**, 021303 (2012).

[24] A. Samadani, A. Pradhan, and A. Kudrolli, Size segregation of granular matter in silo discharges, Physical Review E **60**, 7203 (1999).

[25] Q. Chen, R. Li, W. Xiu, V. Zivkovic, and H. Yang, Measurement of granular temperature and velocity profile of granular flow in silos, Powder Technology **392**, 123 (2021).

[26] I. Zuriguel, D. Maza, A. Janda, R. C. Hidalgo, and A. Garcimartín, Velocity fluctuations inside two and three dimensional silos, Granular Matter **21**, 1 (2019).

[27] D. Walker, An approximate theory for pressures and arching in hoppers, Chemical Engineering Science **21**, 975 (1966).